warwick.ac.uk/lib-publications

Non-linear Signal Detection for Molecular Communications

Bin Li
School of Information and
Communication Engineering (SICE)
BUPT, Beijing, China, 100876

Weisi Guo
School of Engineering,
University of Warwick,
West Midlands, CV4 7AL

Chenglin Zhao
School of Information and
Communication Engineering (SICE)
BUPT, Beijing, China

Abstract—**Molecular communications convey information via diffusion propagation. The inherent long-tail channel response causes severe inter-symbol interference, which may seriously degrade signal detection performances. Traditional linear signal detection techniques, unfortunately, require both high complexity and a high signal-to-noise (SNR) ratio to operate. In this paper, we proposed a new non-linear signal processing paradigm inspired by the biological systems that achieves low-complexity signal detection even in low SNR regimes. First, we introduce a stochastic resonance inspired non-linear filtering scheme for molecular communications, and show that it significantly improves the output SNR by transforming the noise energy into useful signals. Second, we design a novel non-coherent detector by exploiting the transient features of molecular signaling, which are independent of channel response and involves only low-complexity linear summation operations. Numerical simulations show that this new scheme can improve the detection performance remarkably (approx. 7dB gain), even when compared against linearly optimal coherent methods. This is one of the first attempts to demodulate molecular signals from an entirely biological point of view, and the designed non-linear non-coherent paradigm will provide significant potential to the design and future implementation of nano-systems in noisy biological environments.**

Index Terms—**Molecular communications, non-linear filter, stochastic resonance, non-coherent detector, transient features**

I. INTRODUCTION

Molecular communications is prevalent in natural systems that range across multiple transmission distance scales. They enable flexible information transfer in various adverse environments, by encoding information in self-propelled (diffusion-advection) chemical molecules [1], [4]. In contrast to human telecommunication systems, diffusive molecules do not suffer from the propagation restrictions (i.e. diffraction loss and cut-off frequency) which limit electromagnetic waves (EMW) or acoustic waves [3]. As such, molecular communications create a new information delivery framework, which is more effective in harsh biological environments where wave-based signaling may become infeasible. It has wide ranging applications including enabling the Internet-of-Nano-Things (IoNT) in bio precision medicine [17] and industrial sensing. One of the first prototypes was developed in ref. [4], demonstrating that the generic text messages can be delivered along several meters.

In a molecular communication system, three functional components are involved (see Fig. 1), i.e., (1) at a source, information is modulated by chemical molecules; (2) a diffusive channel is responsible for propagating the molecular signals, and (3) a molecular detector is utilized to detect and demodulate the received signals. As a direct result of the functional similarity with telecommunication systems, signal processing techniques developed for the EMW-based communications has been directly used in molecular communications [5], [6], [9]. In [8], coherent detection techniques, such as maximum *a posteriori* (MAP) detector and maximum likelihood (ML) schemes, are applied to combat the diffusion propagation by utilizing the channel state information (CSI).

As far as emerging IoNT applications are concerned, however, such existing linear methods may become less attractive. First, acquiring unknown CSI in diffusion channels is resource demanding and difficult practically. Second, in order to mitigate the inter-symbols interference (ISI), the computational complexity will be unaffordable (i.e., matrix operators for nano-machines is challenging [10]). Last but not least, such linear processing schemes usually require high signal to noise ratios (SNR) to achieve the desired performance, which become impractical in noisy biological environments (constant molecular signaling from multiple sources [7], [21]).

As recognized, various elegant biological mechanisms have been evolved to combat harsh environments [11]. In this work, we proposed a non-linear non-coherent detection scheme for molecular communications. Our non-linear non-coherent signal detection constitutes a new processing paradigm, which is inspired by the long-standing biological concepts and distinguished from the known techniques in EMW communications. The main contributions are summarized as follows:

1) We suggested a non-linear signal filtering mechanism to improve the detection SNR, by constructively exploiting random noises. In contrast to a linear filtering concept, our emphasis, inspired by the biological concept of stochastic resonance (SR), is not just to filter out noise, but also tune it into useful component of output signals.

2) We designed a non-coherent signal detector. Other than focusing on the CSI estimations and channel equalizations, we resort to the inherent *transient* features of filtered waveform. Three independent metrics are thereby constructed, and the signal detection is realized without acquiring CSI.

3) We evaluated the performance of our biologically inspired signal processing scheme. The detection SNR can

be enhanced greatly via the non-linear filtering. Further combined with the CSI independent non-coherent detector, the performance would be significantly improved, even compared to existing linear coherent detectors.

II. SYSTEM MODELS

A. Molecular Communications

Much similar to an EMW-based communication system, a generalized model for molecular communications is shown in Fig. 1 [8], [12].

1) Information source: An information source may be either a single cell/organism in a biological system, or a simple hardware transmitter in artificial system. Rather than EMW carriers, the information will be encoded (or modulated) by molecular amplitude (i.e. concentration) or phase (i.e. interval), as in most biological systems [2]. With the amplitude modulation (AM) [6], the emitted signal is expressed as:

$$s(t) = Q \cdot \sum_{k=0}^{\infty} \alpha_k \cdot \text{rect}\left(\frac{t - T_p/2}{T_p} - kT_b\right). \quad (1)$$

where T_b is the symbol duration and T_p denotes the impulse width. There contains a total of Q molecules at the kth interval if the binary symbol $\alpha_k \in \mathcal{A} = \{0, 1\}$ is 1 ($k = 0, 1, \cdots, \infty$). Here, a rectangular pulse shaper $\text{rect}(\cdot)$ is adopted.

2) Propagation channel: Taking the 1-D free diffusion for example, according to the Fick's second law and subjected to an initial condition $p(x, 0) = \delta(x)$, the expected concentration for the travelling time $t > 0$ and a transmitter-receiver distance d is given by [14]:

$$h(t; d) = \frac{1}{\sqrt{4\pi Dt}} \times \exp[-d^2/(4tD)]. \quad (2)$$

3) Information sink: The sink can be either another cell membrane (e.g. in biological systems) or a hardware receiver (e.g. a molecular sensor in artificial device). At the receiver-end, the observed signal is expressed as:

$$y(t) = s(t) \otimes w(t) + z(t), \quad (3)$$

Here, we consider a linear system model [8], [10], where the notation $\otimes$ denotes the convolution. $w(t) = \text{rect}[(t - T_p/2)/T_p - kT_s] \otimes h(t)$ gives the equivalent channel between the binary information source $\{\alpha_k\}$ and a nano-receiver, as in Fig. 1-(a). $z(t)$ accounts for the additive noise induced by the imperfect counting process or other environmental disturbances, which is modeled as the i.i.d white Gaussian noise, with a variance of σ_z^2, i.e. $z(t) \sim \mathcal{N}(0, \sigma_z^2)$.

B. Equivalent Discrete Signals

At the receptor, a detector will sample the concentration of signaling molecules with the Nyquist rate $R = 1/T_b$ [8], [10]. After doing so, the discrete signal becomes:

$$y_k = \sum_{l=0}^{\infty} \alpha_l \times w_{k-l} + z_k, \quad (4)$$

where $y_k = y(kT_b)$, $w_k = w(kT_s - lT_b)$ and $z_k = z(kT_b)$. For a causal system, we have $w_{k-l} = 0$ if $k - l < 0$.
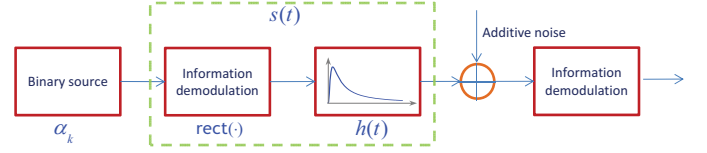

Fig. 1. A shared schematic structure of both EMW-based communications and molecular communications.

Without losing generality, here we assume the synchronization has been accurately accomplished via specific techniques [13]. Furthermore, the discrete signal is re-formatted to:

$$y_k = \alpha_k w_k + \sum_{l=k-1}^{I} \alpha_l w_{k-1-l} + z_k, \quad (5)$$

Due to the long-tail channel response, serious ISI will be inevitable, as in the second term on the right of Eq. (5). Without the loss of generality, a finite ISI length I is assumed.

C. Linear & Coherent Methods

1) MAP detector: For convenience, a vector expression of received signals is further written as $\mathbf{y} = \mathbf{W}\boldsymbol{\alpha} + \mathbf{z}$, where $\mathbf{y} = [y_0, y_1, \cdots, y_K]^T$, $\mathbf{W}$ denotes a circulant channel matrix constructed from $\mathbf{w}$, while $\mathbf{z}$ is the noise vector. In general, an MAP detector aims to maximize the *a posteriori* probability dentistry function (PDF) of unknown information symbols conditioned on the received samples, i.e.,

$$\hat{\boldsymbol{\alpha}}_{\text{MAP}} = \arg \max_{\boldsymbol{\alpha} \in \mathcal{A}^K} P(\boldsymbol{\alpha}|\mathbf{y}, \mathbf{W}),$$

$$= \arg \max_{\boldsymbol{\alpha} \in \mathcal{A}^K} \prod_{k=0}^{K} p(\alpha_k|\alpha_{0:k-1}) \prod_{k=0}^{K} P(y_k|y_{0:k-1}, \alpha_{0:k}). \quad (6)$$

Given the i.i.d Gaussian noise, the likelihood densities $p(y_k|y_{0:k-1}, \alpha_{0:k})$ follow the Normal distributions [8]. In the above coherent MAP, the accurate estimation of CIR will be indispensable in evaluating likelihood densities. As seen, the complexity of such an MAP scheme comes from the sequential evaluation of likelihood densities [10].

2) MMSE detector: Another popular linear detector is inspired by the MMSE criterion, which aims to minimize the covariance matrix of detection errors, i.e.,

$$\hat{\boldsymbol{\alpha}}_{\text{MMSE}} = \arg \max_{\boldsymbol{\alpha} \in \mathcal{A}^K} \mathbb{E}\left[(\boldsymbol{\alpha} - \hat{\boldsymbol{\alpha}})(\boldsymbol{\alpha} - \hat{\boldsymbol{\alpha}})^T\right]. \quad (7)$$

Based on the linearly Gaussian model as in (5), the MMSE estimation is derived via:

$$\hat{\boldsymbol{\alpha}}_{\text{MMSE}} = \mathbb{E}(\boldsymbol{\alpha}|\mathbf{r}),$$

$$= \mathbb{E}(\boldsymbol{\alpha}) + \boldsymbol{\Gamma}_z \mathbf{W}^T (\mathbf{W}\boldsymbol{\Gamma}_z \mathbf{W}^T + \boldsymbol{\Gamma}_z)^{-1}(\mathbf{y} - \mathbf{W}\boldsymbol{\alpha}), \quad (8)$$

where $\mathbb{E}(\cdot)$ represents the statistical expectation, $\boldsymbol{\Gamma}_z$ is an $K \times K$ diagonal matrix with its elements are all σ_z^2. For the above MMSE scheme, the accurate CIR will be indispensable.

III. NONLINEAR FILTERING

A. Nonlinear vs Linear Filtering

In order to suppress the environmental noise, a filtering process will be necessary, especially in low SNR region. When it comes to the well-studied linear filters, e.g. finite impulse response (FIR) filter, the distortion of output signals will be inevitable (in Fig. 3), due to the non-sharp frequency transitional property. Meanwhile, such FIR schemes incur also the high complexity in hardware/mechanical implementations (e.g. hundreds of delayed taps).

Inspired by biological or physical mechanisms, a non-linear filtering scheme, in contrast, is premised on specific stochastic PDE (SPDE), which has the potential of suppressing useless noises whilst enhancing useful signals. In the following, we resort to the non-linear SR mechanism to process noisy signals. First, we will shortly elaborate the basic principle of SR. Then, we will discuss the implementation and configuration issues of our non-linear filtering scheme.

B. Stochastic Resonance

1) Basic Principle: The concept of SR is originally proposed by Benzi and collaborators when studying the periodically recurrent ice ages [15]. According to [15], [16], an extra dose of noise could help rather than hinder the performance in some cases. To be specific, we then consider the following stochastic dynamical system driven by a weak input $A_0 \times \cos(\Omega t + \varphi)$, i.e.

$$\frac{dx(t)}{dt} = -\frac{dV(x)}{dx} + A_0 \cdot \cos(\Omega t + \varphi) + \sqrt{D}\xi(t), \quad (9)$$

where $x(t)$ is the output state, and $\xi(t)$ is the additive i.i.d Gaussian noise with the variance of D. The above dynamical system is governed by a double-well potential $V(x)$:

$$V(x) = -a/2 \cdot x^2 + b/4 \cdot x^4, \quad (10)$$

which has two minima located at $x_m = \pm\sqrt{a/b}$, corresponding to two stable states. The potential barrier, with the barrier height of $\Delta V = a^2/4b$, is located in the middle of two stable states. A unstable local maximum is located at x_b=0.

With the suitable dose of noises, the potential barrier will be biased, and the system outcomes $x(t)$ may transit to two states with different likelihoods. Once the synchronization between the noise-induced transitions and the external input is achieved, the system outcome will be significantly enhanced. Given the initial condition $x_0 = x(t)|_{t=t_0}$, then the output response is given by [16]:

$$\lim_{t_0 \to -\infty} \langle x(t)|x_0, t_0 \rangle = \bar{x}(D) \times \cos[\Omega t - \bar{\varphi}(D)]. \quad (11)$$

Here, $\langle x \rangle$ gives the conditional and ensemble averaging of $x(t)$ over noises [16]. From eq. (11), the output response is also a periodic signal, sharing the same frequency with the weak input forcing, i.e., Ω. However, the amplitude as well as its phase are now mediated by the noise variance D as well as the underlying potential function (a and b), i.e. $\bar{x}(D) = A_0 x_m^2/D \times \frac{2r_0}{\sqrt{4r_0^2 + \Omega^2}}$, $\bar{\varphi}(D) = \arctan(\Omega/2r_0)$.
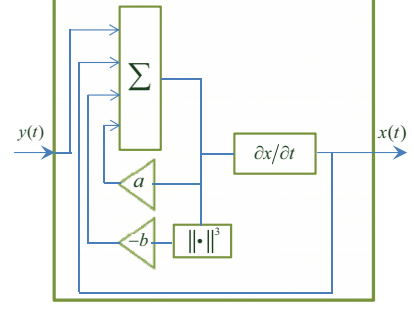

Fig. 2.   A schematic structure of non-linear filter in the analog domain.

It is shown that there exists an optimal noise variance that maximizes the output SNR. In practice, a too small noise variance will be insufficient to lead a state crossing the potential barrier even biased by input force. Yet, a too large noise variance may put the state transition into random jumps, which may overwhelm the input periodic forcing [16].

C. Implementations

Relying on the above analysis, we then utilize a nonlinear SR mechanism to denoise molecular signals. As illustrated by Fig. 2, the received signal $y(t)$ (or y_k) will be fed directly into a tuned SR system. Then, its output $x(t)$ (or x_k) will tend to be a noise-reduced and signal-enhanced version of input noisy signal.

1) Analog domain: It is revealed that the nonlinear SR mechanism occurs widely in biological systems. For example, relying on the dynamical kinetics of reactions (a group of differential equations), the ion channels in cell membrane can amplify the signaling in vitro, with the help of noise effects even in harsh biological environments. For the concerned molecular communications, an efficient schematic structure for analog SR processing is shown in Fig. 2. Thus, we may conclude that the SR mechanism can be implemented simply, which, for example, involves a differentiator, an adder, two amplifiers and a power operator.

2) Digital domain: In some applications, the digital implementation will be preferable, e.g. when developing a non-linear filter in small-size chips. In this case, one has to solve the SPDE in Eq. (9), probably with the help of high-performance computations. We employ the fourth-order Runge-Kutta method (RKM) [18], which approximates numerically the solution of SPDE. Relying on the *mean value theorem* of difference, the RKM will approximate the output $x_{k+1} = x[(k+1)\Delta t]$ via the current one $x_k = x(k\Delta t)$, i.e., $x_{k+1} - x_k = x'(\varepsilon)\Delta t$ with $\varepsilon \in [k\Delta t, (k+1)\Delta t]$. Let $\rho = \Delta t$, then next outcome state will be estimated via:

$$x_{k+1} = x_k + \frac{1}{6} \times (q_1 + 2q_2 + 2q_3 + q_4), \quad (12)$$

where each increment term is calculated via:

$$q_1 = \rho \times (ax_k - bx_k^3 + y_k), \quad (13)$$

$$q_2 = \rho \times \left[a \cdot \left(x_k + \frac{q_1}{2} \right) - b \cdot \left(x_k + \frac{q_1}{2} \right)^3 + y_{k+1} \right], \quad (14)$$
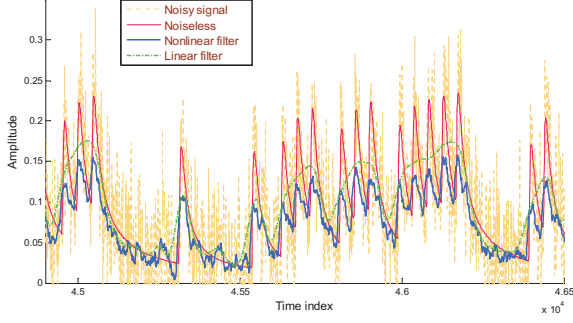
Fig. 3. Time waveform of the received noisy signals and noiseless signals. Here, the finite impulse response (FIR) filter is used, where the Kaise windowing is used, the passing band is configured to 0.224×10^9Hz while the stopping band is about 1×10^9Hz. Given the ripple of passing band 0.01, then the order of FIR filter is about 144.

$$q_3 = \rho \times \left[a \cdot \left(x_k + \frac{q_2}{2} \right) - b \cdot \left(x_k + \frac{q_2}{2} \right)^3 + y_{k+1} \right], \quad (15)$$

$$q_4 = \rho \times \left[a \cdot \left(x_k + \frac{q_3}{2} \right) - b \cdot \left(x_k + \frac{q_3}{2} \right)^3 + y_{k+1} \right]. \quad (16)$$

Here, the iteration step ρ is related to the sampling frequency. The higher the sampling rate, the smaller the iteration step, and the smaller the residua error which is measured as $o(\rho^5)$. However, a small ρ may lead to slow update.

D. Output Analysis

The output signal after non-linear filtering is shown in Fig. 3. We see that the noise in output signls has been effectively suppressed. More importantly, in contrast to the outputs of a linear filtering whereby the local undulation of input signals have been smoothed out, the subtle transient features that will be of significance to subsequent information demodulation are reserved completely.

When configuring the above nonlinear system, we consider the special case $A_0 = 0.5 \times \sqrt{4a^3/(27b)}$ [19] and $\Delta V = D$. Thus, the feasible parameters can be configured as $a = \frac{27 \times (2A_0)^2}{16D}$, $b = \frac{a^2}{4D}$. Notice that, for the concerned molecular signals (which is always positive), we approximate the signal amplitude with $A_0 \simeq \mathbb{E}\{y(t)\}$. Meanwhile, it may become impossible to know the realistic noise variance. As an alternative, one may tend to the performance optimization of the high SNRs (e.g. SNR*=5dB) and, therefore, the noise variance will be prescribed to $D = D_{\text{est}} = 10^{-\frac{\text{SNR}^*}{10}} \times A_0$.

IV. NON-COHERENT DETECTIONS

In contrast to the CSI-dependent coherent detectors (e.g. MAP and MMSE), we then designed a non-coherent detection scheme by exploring the transient features of molecular signals. Such a transient-feature detection concept is inspired by biological mechanisms in cell signaling, e.g., different concentration gradient slopes trigger various responses [20].

A. Metric Construction

In the non-coherent detection framework, the decision metric is constructed directly from filtered response $x(t)$ (or x_n), which hence exclude the estimated CSI completely.
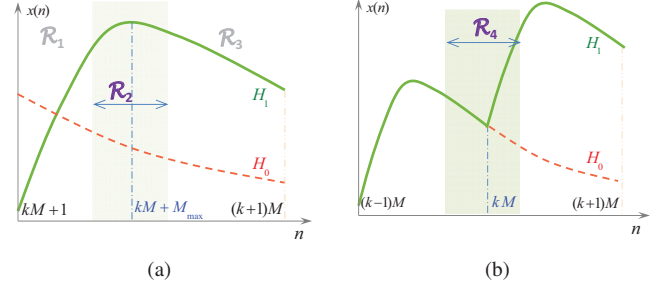

Fig. 4. Transient characteristics of filtered signal response.

To be specific, we have defined three decision sub-metrics by respectively exploring: (1) the local geometry shape in each symbol, (2) the transient property among two adjacent symbols, and (3) the energy difference between two symbols.

1) Local geometry shape: Taking the kth interval with $M = T_b f_s$ samples for example, in the case of H_1 (i.e. α_k=1) the output $x(n)$ will firstly arise until its maximum (located at $M_x \triangleq kM + M_{\max}$), then it will decay slowly. As in Fig. 4-(a), the output response in a region $\mathcal{R}_2$ will be higher than its left neighbor region $\mathcal{R}_1$ and its right neighbor region $\mathcal{R}_3$. In practice, we will specify the width of $\mathcal{R}_2$ to be $M/4$, i.e. the half length $L_0 = M/8$. Thus, the first metric is defined as:

$$c_{k,1} = \frac{1}{2L_0 + 1} \cdot \sum_{n=M_x-L_0}^{M_x+L_0} x_n +$$

$$\frac{1}{2} \cdot \frac{1}{M - 2L_0 - 1} \cdot \left(\sum_{n=kM}^{M_x-L_0-1} x_n + \sum_{n=M_x+L_0+1}^{(k+1)M-1} x_n \right).$$
(17)

It is easily noted that, in the case of H_1 (i.e. α_k=1) $c_{k,1}$ will be larger than 0. Otherwise, it may be smaller than 0 in the case of H_0 (i.e. α_k=0). So, it can be indeed used as a metric to justify whether there are new molecules arrives at a receptor at current interval.

2) Transient shape among symbols: When it comes to two successive slots k and $k + 1$, the transient shape at the beginning of the next symbol (i.e. kM) will be quite different in two cases (i.e. H_1 and H_0), see Fig. 4-(b). To be specific, in the case of H_0 (α_k=0), the output response will continue to decay in the following time. In contrast, for H_1 (α_k=1) an obvious inflection may occur. To exploit such a transient pattern, another metric is defined as:

$$c_{k,2} = \frac{-1}{2L_1 + 1} \cdot \sum_{n=kM-L_1}^{kM+L_1} x_n +$$

$$\frac{1}{2} \cdot \frac{1}{2L_2 + 1} \cdot \left(\sum_{n=kM-L_1-L_2}^{kM-L_1-1} x_n + \sum_{n=kM+L_1+1}^{kM+L_1+L_2} x_n \right).$$
(18)

where L_1 will be configured to a small value, i.e. $L_1 = 1$.

3) Energy difference: Except for the above two sub-metrics, another differential metric can be also used, which utilizes the concentration difference induced by the new arrived

molecules and exploits the slow-decay property of diffusion channels. Thus, the third metric is defined as:

$$c_{k,3} = \frac{1}{M} \cdot \sum_{n=kM+1}^{(k+1)M} x_n - \frac{1}{M} \cdot \sum_{n=(k-1)M+1}^{kM} x_n. \qquad (19)$$

Finally, the compound non-coherent metric is given by:

$$c_k = c_{k,1} + c_{k,2} + c_{k,3}. \qquad (20)$$

As elaborated above, the designed metrics are consistent in detecting the new arrived molecules, i.e., $c_{k,i} \underset{\alpha_k=1}{\overset{\alpha_k=0}{\lessgtr}} \lambda$ ($i = 1, 2, 3$). More importantly, with the independent noise samples, the combination of the above three sub-metrics further provides the extra gain in detection performances.

B. Detection Threshold

Since the noise samples of various discrete time remains independent, c_k will be Gaussian distributed when the sample size M is sufficiently large (e.g. ≥ 20), according to the central limit theorem (CLT). Conditioned on the different information bit (i.e. H_1 or H_0), the likelihood densities of the designed metric are:

$$p(c_k|H_1, t_0 \to -\infty) \sim \mathcal{N}(E_1, \sigma_c^2), \qquad (21)$$
$$p(c_k|H_0, t_0 \to -\infty) \sim \mathcal{N}(E_0, \sigma_c^2). \qquad (22)$$

Here, $E_0 \triangleq \mathbb{E}(c_k|H_0, t_0 \to -\infty)$, and the distribution variance σ_c^2 will be related with the sample size M, and the residual noise variance in x_k.

Then, a threshold λ can be derived according to certain criterion, e.g. the minimum detection errors (MDE), with which the estimation of unknown symbols is derived via:

$$\hat{\alpha}_k = \begin{cases} 1, & c_k \geq \lambda, & (23a) \\ 0, & c_k < \lambda. & (23b) \end{cases}$$

With the equal prior (i.e. $p(H_0) = p(H_1) = 0.5$) and in the absence of extract distribution parameters (i.e. E_1 and σ_c^2), a feasible approach is to update the threshold adaptively according to:

$$\lambda_k = (1 - \beta) \times \lambda_{k-1} + \beta \times \frac{1}{k} \sum_{k'=1}^{k} c_{k'}, \qquad (24)$$

where β is a forgotten parameter which is ranged in $[0.9, 0.99]$; an initial threshold estimation can simply be set to $\lambda_0 = 0$. It is shown that, as an iteration number k increases, the estimated threshold will converge to the optimal MDE threshold, i.e.,

$$\lim_{k \to \infty} \lambda_k = \frac{1}{k} \sum_{k'1=1}^{k} c_{k'} \simeq \mathbb{E}(c_k),$$
$$= p(H_1) \times \mathbb{E}(c_k|H_1) + p(H_0) \times \mathbb{E}(c_k|H_0),$$
$$= \lambda_{\text{opt}}. \qquad (25)$$

V. NUMERICAL SIMULATIONS

In this section, we will evaluate the detection performance of our proposed non-linear non-coherent detector. In the following simulations, the diffusion constant is set to $C = 7 \times 10^{-9}$, and $d = 9 \times 10^{-9} m$, $T_s = 1/f_s = 2 \times 10^{-10}$ sec, $T_b = 9 \times 10^{-9}$ sec. That is, the discrete samples within each symbols duration is M=45.
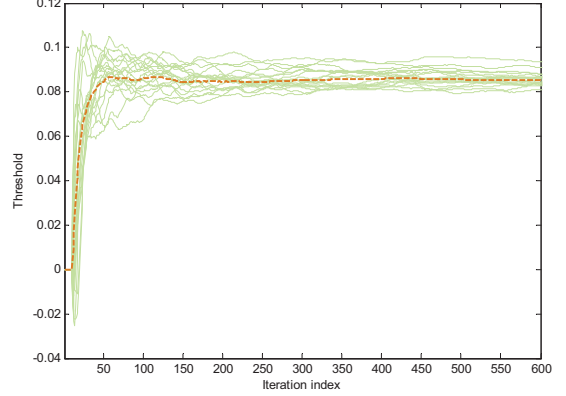

Fig. 5. Threshold adaption of 20 independent realizations (*Dotted*: average).

A. Adaptive Threshold

First, we studied the proposed adaptive threshold mechanism in Eq. (24). When the input SNR is configured to 8dB, the adaptive thresholds obtained from 20 independent realizations are plotted together in Fig. 5. It is seen that the threshold can be determined numerically via the decision variables c_k ($k = 0, 1, 2, \cdots, K-1$), and its convergence can be achieved after around 60 symbols (corresponding to the start-up time). From the BER performance, the unknown binary signals can be detected correctly via our designed threshold, even in the initial start-up stage. Thus, with the non-coherent decision metric and the designed adaptive threshold, our new algorithm would exclude CSI accompanying its complex estimation.

B. Performance Comparison

Then, we compare the detection performance of our new scheme with other existing methods. Two counterparts are considered here, i.e. the coherent MAP detection and the non-coherent detection (which is similarly based on local convexity) [10]. For the MAP scheme, we assume the diffusive CSI $h(t)$ has been accurately estimated, which may additionally consume the considerable time (e.g. dedicated pilots carrying no information is required to estimate CSI) and computation resource (e.g. frequently evaluating the likelihoods). In all cases, we assume the accurate timing has been acquired.

From Fig. 6, we noted that, with the linear processing framework, the MAP detector can obtain the optimal performance, in the sense that it fully exploited the statistics of observations and CSI. However, it requires the accurate CSI estimation and complex computations, and tends to be less attractive low-power and low-complexity applications. The linear non-coherent detector in ref. [10] relies similarly on the convexity shape of molecular concentration, which will effectively alleviate the computation burden and hence is applicable to low-complexity scenarios. However, such two linear detectors acquire satisfactory performances only in high SNRs (e.g. >12dB), which, unfortunately, becomes impractical in noisy and disturbing biological environments.

In comparison, our proposed non-linear non-coherent detector provides the great promise to molecular communications.
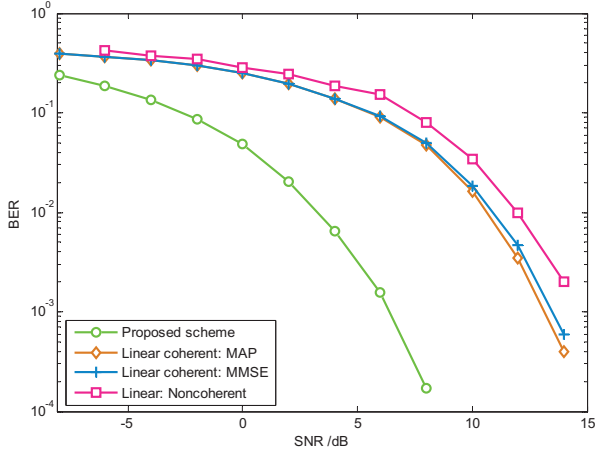
Fig. 6. BER performance of various detection methods.

For one thing, it excludes complicated CSI estimation and complex computations, and its implementations will be very simple (e.g. Fig. 2), which greatly facilitates the emerging nano-scale communications. For another, the random noise can be utilized constrictively, which further contributes to improve the output SNR. Thus, the non-linear filtering dramatically outperforms the existing linear filtering schemes. From Fig. 6, a rough detection gain of 7dB can be achieved via the proposed non-linear non-coherent detector, even compared against the optimal linear detector. Thus, our new non-linear non-coherent processing paradigm will be of significance to molecular communications, especially for IoNT systems in harsh biological environments.

VI. Conclusions

Through long-term competitive evolution, biological systems have created their own effective signal processing mechanisms [11]. Although some of them remain elusive, such methods, e.g. usually nonlinear and dynamically complex, have been demonstrated to be successful in various noisy biological environments (e.g. Fig. 5). In some cases, applying the popular concepts/techniques developed for EMW communications directly to molecular communication will be proved of little avail, or even might have just the opposite effect (e.g. increased complex and reduced performance).

Inspired by biological principles, we proposed a non-linear non-coherent signal processing scheme based on stochastic resonance (SR). The concept of SR is exploited to perform non-linear filtering, which not only can filter out noise but also transform the noise energy into useful signals via specific non-linear dynamical mechanisms. In this paper, a novel non-coherent detector is designed, which fully utilize the transient features of molecular signaling. It is shown that, with the new non-linear and non-coherent paradigm, the detection performance can be improved by 7dB compared with an optimal coherent detector. This is one of the first attempts to design bio-signaling inspired filters for molecular communications, and it may provide us with a new perspective from both bio-signaling and telecommunications perspectives.

References

[1] T. D. Wyatt, "Fifty years of pheromones," *Nature*, vol. 457, 2009, pp. 262-263.

[2] J. Purvis, and G. Lahav, "Encoding and Decoding Cellular Information through Signaling Dynamics," *Cell*, vol. 152, no. 5, 2011, pp. 945-956.

[3] W. Guo, C. Mias, N. Farsad, and J. L. Wu, "Molecular versus Electromagnetic Wave Propagation Loss in Macro-Scale Environments," *IEEE Transactions on Molecular, Biological and Multiscale Communications*, vol. 1, no. 1. 2015, pp. 18-25.

[4] N. Farsad, W. Guo, and A. W. Eckford, "Tabletop molecular communication: Text messages through chemical signals," *PLOS ONE*, 2013, vol. 8, no. 12, e82935.

[5] B. Li, M. Sun, S. Wang, W. Guo, C. Zhao, "Low-complexity Noncoherent Signal Detection for Nano-Scale Molecular Communications," *IEEE Transactions on NanoBioscience*, vol. 15, no. 1, 2015, pp. 3-10.

[6] W. Guo, T. Asyhari, N. Farsad, H. B. Yilmaz, B. Li, A. Eckford, C-B. Chae, "Molecular Communications: Channel Model and Physical Layer Techniques," *IEEE Wireless Communications*, vol. 23, no. 4, 2016, pp. 120-127.

[7] B. Atakan, O. B. Akan, and S. Balasubramaniam, "Body area nanonetworks with molecular communications in nano-medicine," *IEEE Communications Magazine*, vol. 50, no. 1, 2012, pp. 28-34.

[8] D. Kilinc and O. B. Akan, "Receiver Design for Molecular Communication," *IEEE Journal on Selected Areas in Communications*, vol. 31, no. 12, 2013, pp. 705-714.

[9] A. Noel, K. C. Cheung, and R. Schober, "Optimal receiver design for diffusive molecular communication with flow and additive noise," *IEEE Trans. NanoBiosci.*, vol. 13, no. 3, 2014. pp. 350C362.

[10] B. Li, M. Sun, S. Wang, W. Guo, C. Zhao, "Local Convexity Inspired Low-complexity Non-coherent Signal Detector for Nano-scale Molecular Communications," *IEEE Transactions on Communications*, vol.64, no. 5, 2016, pp. 2079-2091.

[11] M. A. Lemmon, J. Schlessinger, "Cell signaling by receptor tyrosine kinases," *Cell*, 2010, vol. 141, no. 7, pp. 1117-1134.

[12] M. Pierobon and I. F. Akyildiz, "A physical end-to-end model for molecular communication in nanonetworks," *IEEE J. Sel. Areas Commun.*, vol. 28, no. 4, pp. 602C611, May 2010.

[13] H. ShahMohammadian, G. G. Messier, S. Magierowski, "Blind synchronization in diffusion-based molecular communication channels," *IEEE communications letters*, 2013, vol. 17, no. 11, pp.2156-2159.

[14] N. Farsad, N. Kim, A. Eckford, and C. Chae, "Channel and noise models for nonlinear molecular communication systems," *IEEE Journal on Selected Areas in Communications*, vol. 32, no. 12, 2014, pp. 1-14.

[15] R. Benzi, G. Parisi, A. Sutera, et al., "Stochastic resonance in climatic change," *Tellus*, 1982, vol. 34, no. 1, pp. 10-16.

[16] L. Gammaitoni, P. Hänggi, P. Jung, et al., "Stochastic resonance," *Reviews of Modern Physics*, vol. 70, no. 1, 1998, pp. 223-287.

[17] I. F. Akyildiz, M. Pierobon, S. Balasubramaniam, Y. Koucheryavy, "The Internet of Bio-Nano things," *IEEE Communications Magazine*, vol. 53, no. 3, 2015.

[18] A. R. Yaakub, D. J. Evans, "A fourth order RungeCKutta $RK(4,4)$ method with error control," *International Journal of Computer Mathematics*, 1999, vol. 71, no. 3, pp. 383-411.

[19] F. Duan, D. Rousseau, F. Chapeaublondeau, "Residual aperiodic stochastic resonance in a bistable dynamic system transmitting a supra-threshold binary signal," *Physical Review E*, 2004, vol. 69, no. 1, pp. 383-391.

[20] J. T. Smith, J. T. Elkin, W. M. Reichert, "Directed cell migration on fibronectin gradients: effect of gradient slope," *Experimental cell research*, 2006, vol. 312, no. 13, pp. 2424-2432.

[21] Y. Deng, A. Noel, W. Guo, A. Nallanathan, M. Elkashlan, "Stochastic Geometry Model for Large-Scale Molecular Communication Systems," *IEEE Global Communications Conference (GLOBECOM)*, 2016.